# Studies on Density, Corrosion Rate and Hardness Characteristics of Stainless Steel Implanted by Nitrogen Ion

IOP Conf. Series: Materials Science and Engineering **515** (2019) 012018 doi:10.1088/1757-899X/515/1/012018

# Studies on Density, Corrosion Rate and Hardness Characteristics of Stainless Steel Implanted by Nitrogen Ion

**Ainun Nikmah**[1,2], **Djoni Izak Rudyardjo**[1], **Jan Ady**[1], **Ahmad Taufiq**[2,*]

[1] Department of Physics, Faculty of Science and Technology, Airlangga University, Jl. Mulyorejo, Surabaya 60115, Indonesia
[2] Department of Physics, Faculty of Mathematics and Natural Sciences, Universitas Negeri Malang, Jl. Semarang 5, Malang 65145, Indonesia

*Corresponding author's email: ahmad.taufiq.fmipa@um.ac.id

**Abstract:** In this work, the surface treatment of stainless steel 304 was conducted using nitrogen an ion implantation route performing at 90 KeV and 100 μA with a dose variation of $0.7\times10^{17}$, $1\times10^{17}$, $1.3\times10^{17}$, and $1.6\times10^{17}$ atoms/cm$^2$. The stainless steel used was a thin plate with a thickness of 2 mm and a diameter of 14 mm. The data analysis showed the sample density increased with the increase of nitrogen ions. The samples had hardness value up to 143.32 HVN at an optimum dose of $1\times10^{17}$ ions/cm$^2$. Such an increase is predicted due to the formation of a new nitride layer on the surface. Furthermore, the corrosion properties showed that the best corrosion resistance was of 0.71 mm/year. The microscope electron investigation presented the addition of nitrogen ions.

**Keywords:** Stainless steel 304, nitrogen ion implantation, density, hardness, nitride layer.

## 1. Introduction

The increasing number of medical needs from time to time for bone graft has encouraged the researchers to try to conduct a biomaterial development with various material engineering methods [1]. Based on the literature, the increase in the number of grafting surgery is estimated to reach 607% between 2005 and 2030 [2]. Therefore, the material development is vital to sustain. The development is expected to be able to produce more durable biomaterials and has excellent hardness properties, biocompatible, wear resistance, and corrosion resistance.

Metal is one of the biomaterials used in diverse medical applications due to its outstanding mechanical properties, wear resistance, hardness, and high strength [3,4]. Metal biomaterials typically used for medical application among them are stainless steel, CoCr alloy (cobalt-chromium) and chromium, and 1.2% carbon [5]. The utilization of stainless steel has been employed for various medical applications such as orthopedics, cardiovascular, craniofacial surgery, otorhinolaryngology applications, hip implant stems, coronary stents, and spinal disc replacements [3,6]. The commonly used stainless steel for medical applications is stainless steel 316L. However, the high cost of stainless steel 316L becomes an issue in the medical world and eventually becomes the consideration of replacing it with stainless steel type 304 [7].

Stainless steel 304 is a type of stainless steel austenitic which has a structure of FCC (Face Center Cubic) and paramagnetic properties. Stainless steel 304 has a higher corrosion resistance than ordinary steel. This steel contains 0.0025% sulphur , 0.0075% phosphor, 0.4 % silicon, 1.24 % manganese, 0.06 % carbon, 8.8 % nickel and 18,5 % chromium [8]. Stainless steel 304 is also often used in the medical application because of its high tenacity, corrosion resistance, and a strong mechanical property [8,9]. However, for a very acidic environment, stainless steel corrosion resistance decreases, whereas the very acidic human body environment can lead to corrosion and protein adsorption. Besides, the main weakness of this material is its low hardness, which results in poor tribology property [10]. Therefore, the treatment surface effort needs to be performed to increase the mechanical property from this material. Numerous methods can be used to increase the austenitic steel's mechanical characteristic. One of them is by ion implantation [11–14], saddle field fast atom beam source [15–17], sputtering [18–20], and active screen plasma nitriding [21–23]. In this research, we utilize an ion implantation method due to its advantages among them are not altering dimension [24]. Insertion (depth) can be controlled by adjusting the voltage, and the neutralization process is clean because it is done in a vacuum space [25]. Another advantage is not involving the heat substance thus the possibility of thermal stress incidence which can cause a dimension alteration can be avoided.

Ion implantation is a method of adding or penetrating ion into the material which functions as a tool to modify a biomaterial surface [26]. Ion implants are also generally used for doping of semiconductor devices that to modify the surface of materials. In the ion implantation process, energy ions penetrate to the surface of the materials and interact with the substrate of materials. In general, the changes in composition tend to produce new phases and surface hardening [24]. Based on the previous research, nitrogen ion implantation is proven to affect the increase in wear resistance of prostatic components such as knee and hip grafting [27]. Ion implantation is affected by ionic dose and energy. The ion dose will affect the number of ions fired into the material. Meanwhile, ionic energy will affect the depth of the ion passing through the material. In such process, the nitrogen atom is ionized and then accelerated thus it can penetrate the surface layer that will be implanted.

Several studies showed that nitrogen ion implantation could increase material tribology properties such as hardness, wear resistance, and corrosion resistance [26–29]. Some elements such as N, Ti, and Cr increase the occurrence of phase formation and microstructure alteration, as well as the chemical and mechanical properties. However, among those ions, the ion that is very appropriate for biomedical application is nitrogen ion [26]. Nitrogen element is an interstitial solute which can contribute to the formation of the austenitic phase [30]. Some researchers also state that the addition of nitrogen ions can lead to the formation of iron nitride phases on the surface, which will cause a significant increase in abrasive wear, wear fatigue, and erosion when they experience conditions of increased hardness on the surface [31].

Another group conducted a study of nitrogen ion implantation on stainless steel, obtained the best corrosion resistance at a dose of $5 \times 10^{18}$ ion/cm$^2$ with a corrosion current density of 81.4 μAcm$^{-1}$ [5]. Padhi *et al*. [32] have reported nitrogen ion implantation on 304 stainless steel having the best corrosion resistance at a dose of $2.5 \times 10^{17}$ ions/cm$^2$. The results of nitrogen ion implantation on 304 stainless steel successfully inhibited direct contact between corrosive ions and the sample surface, so that the corrosion resistance increased. However, based on our knowledge, the use of 304 stainless steel for the medical field is rarely studied. So far 304 stainless steel applications have only been applied to the industrial sector because the corrosion rate of stainless steel is still relatively high to be applied in the medical application. Therefore, in this study, we examined the potential of 304 stainless steel for medical applications using the nitrogen ion implantation method. The purpose of this study was to determine the effect of variations in nitrogen ion dosage on the characteristics of 304 stainless steel as a candidate for medical material.

## 2. Methods

The materials used in his study were stainless steel 304, gas nitrogen, autosol, water, alcohol 96% and SBF solution (Simulation Body Fluid). The first process was sample preparation where stainless steel was cut into disk shapes with a thickness of 2 mm and a diameter of 14 mm. The sample was refined using a polishing machine and diamond paste. After polishing, the sample was cleaned with an ultrasonic machine in alcohol and then dried. Then, stainless steel 304 was implanted with nitrogen ions performed at 90 KeV energy Proses. The projected depth (*Rp*) was 995 Å with the standard deviation of the ion distribution projection ($\sigma Rp$) valued until 499 Å (calculated with STRIM program).

The dosage variation in this research is shown in Table 1. Ion dosage is defined by Equation 1 [33], where $D$ is ion dosage, $I$ is current (μA), $e$ is electron charge ($1.6\times10^{-19}$ C), $t$ is implantation time (second), and $A$ is the area ($cm^2$).

$$D = \frac{it}{eA} \tag{1}$$

The sample characterization used was density testing using an Archimedes' principle adjusted with the standard of ASTM A378-88 testing [34]. The potentiostatic polarization method was used for corrosion testing; measurements were made with working electrodes from -2500 mV to +1000 mV with a scan level of 20 mV per second in the medium of the SBF solution (Simulation Body Fluids). The composition of the SBF solution is presented in Table 2. The hardness testing was investigated using Vickers micro testing which employed the force of 3 gf. This case aimed to make the indenter right on target on the area where ion implantation occurred. The microstructure and the element composition was conducted with SEM – EDX testing.

**Table 1**. The variation of nitrogen ion dosages in the implantation process

| Ion Dose (ions/$cm^2$) | Current (μA) | Time (minutes) |
|---|---|---|
| Raw material | - | - |
| $0.7\times10^{17}$ | 100 | 25 |
| $1.0\times10^{17}$ | 100 | 35 |
| $1.3\times10^{17}$ | 100 | 45 |
| $1.6\times10^{17}$ | 100 | 55 |

**Table 2.** The chemical composition of simulated body fluid (SBF)

| Reagent | Amount ($g.L^{-1}$) |
|---|---|
| NaCl | 8 |
| $C_6H_{12}O_6.H_2O$ | 2 |
| $MgSO_4.7H_2O$ | 0.20 |
| $NaHCO_3$ | 0.35 |
| $KH_2PO_4.3H_2O$ | 0.06 |
| $CaCl_2.2H_2O$ | 0.14 |
| $Na_2HPO_4.2H_2O$ | 0.06 |
| KCl | 0.40 |

## 3. Results and Discussion

The density testing was carried out to determine the particle density in the space after nitrogen ion implantation. The value of material density from the data analysis is shown in Table 3. The calculation of material density value used Equation 2 [34].

$$\rho_{archimedes} = \frac{m_{air}}{m_{liquid}} \rho_{liquid} \quad (2)$$

where $\rho_{archimedes}$ is implanted material density (g/cm$^3$), $m_{air}$ is the sample mass in the air (gram), $m_{liquid}$ is the sample mass in the liquid substance (g) and $\rho_{liquid}$ is the water density at the pressure of 1 atm and the temperature of 288.15 K (g/cm$^3$). The analysis of density testing showed that the addition of mass due to nitrogen dopant ions diffuses on the surface of the sample. Mass increase per unit volume will increase the value of material density. The graph of the relationship of density with ion doses is presented in Figure 1.

From the graphic of the relationship between dosage and density, there was a density increase with the increase in ion dosage given. When ion production increases, the ion flux density will also increase on the surface of the substrate, facilitating the rapid penetration of nitrogen atoms into the material. In the ion implantation process, the ions entering the target will lose energy and occupy the target atom's empty space so that the material density increases, and this will increase the material's durability [35].

**Table 3**. The results of density from unimplanted and implanted nitrogen ion

| Ion Dose (ions/cm$^2$) | Density (gram/cm$^3$) |
|---|---|
| Raw Material | 7.9022 ± 0.0024 |
| $0.7\times10^{17}$ | 8.1063 ± 0.0009 |
| $1.0\times10^{17}$ | 8.1265 ± 0.0008 |
| $1.3\times10^{17}$ | 8.1324 ± 0.0004 |
| $1.6\times10^{17}$ | 8.1409 ± 0.0005 |

The increase in density on the unimplanted material with the implanted material was deemed very significantly. This is because, in the implanted sample, the ion diffused between the target atoms (stainless steel 304) and the mass increased. The sample mass with a fixed volume increased due to the diffusion of ions into the empty space of the material. However, the increase in density between doses of $0.7\times10^{17}$ ions/cm$^2$ to a dose of $1.7\times10^{17}$ ions/cm$^2$ was not too high, because the different amount of penetrating ion was only $0.3\times10^{17}$ nitrogen ion per 1 cm$^2$ from the sample area in each of the dosage variations.

The hardness from the material was investigated using Vickers hardness testing, the pounder used was a diamond pyramid with the comparison of its square base and the diagonal length was 1:1. The Vickers testing was used to find out the effect of dosage variation on the material hardness. The calculation of Vickers hardness used Equation 3 [36].

$$HVN = 1.854 \frac{P}{L^2} \quad (3)$$

where VHN is the material hardness value, $P$ is applied weight load (gram force), and $L$ is the average diagonal length (μm).

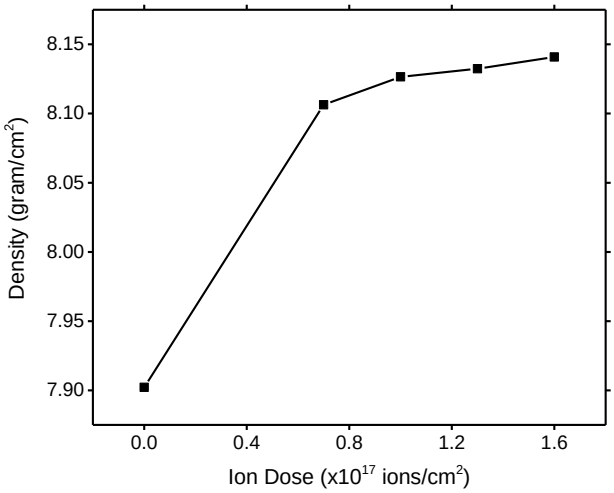


**Figure 1**. The graphic of the relationship between ion dosage variation and material density

The results of the calculation of the hardness value based on the Vickers test are presented in Table 4. Compared to the unimplanted material, the implanted material experiences increased hardness. According to the literature, an increase in nitrogen content qualitatively leads to an increase in the hardness of the modified surface layer [11]. The increased surface hardness in the ion implantation process occurs because of the increase in atomic density in the target material. The combination of energy and ionic doses during the implantation process can shift and release atomic bonds in the material. Thus, there is a defect in the form of a vacancy which is then penetrated by the implanted nitrogen ion. From this phenomenon, the new arrangement of an atom is more dense and free from vacancy defect. The perfect atom position will be able to defend the outer penetration; thus the hardness value of the material increases [35]. Another literature also explained that the sample hardness increases because of the formation of a new nitride layer on the material surface due to the ion implantation [26]. The presence of interstitial nitrogen ions into the target material enables nitrogen ions to interact and bind strongly to the Fe atom on the surface of the substrate to produce a layer of iron nitride (Fe-N) which has harder properties on the material surface. Based on calculations, hardness, a surface layer of material increased up to 35% from 92.4 HVN of pure material to 143.32 HVN.

**Table 4**. The results of Vickers hardness from unimplanted and nitrogen ion implanted

| Ion Dose (ions/cm$^{2)}$ | Vickers Hardness (HVN) |
|---|---|
| Raw material | 92.40 ± 6.43 |
| $0.7\times10^{17}$ | 118.06 ± 2.41 |
| $1.0\times10^{17}$ | 143.32 ± 5.35 |
| $1.3\times10^{17}$ | 108.30 ± 6.52 |
| $1.6\times10^{17}$ | 100.58 ± 2.76 |

The graphic of material hardness due to ion implantation is shown in Figure 2. From this graph, it can be observed that the optimum hardness of SS 304 material planted occurred at an ion dose of $1.0\times10^{17}$ ions/cm$^2$. The addition of ion doses between $1.3\times10^{17}$ - $1.6\times10^{17}$ atoms/cm$^2$ caused the hardness of the material to decrease. The excessive ion dose is not advantageous in the nature of violence due to the nitride phase that has been formed can be broken to form an amorphous phase [31]. From the graphic,

it can be observed that the optimum hardness from the implanted SS 304 material occurred at the ion dosage of $1.0\times10^{17}$ ions/cm$^2$. The addition of ion dosage between $1.3\times10^{17}$ – $1.6\times10^{17}$ atoms/cm$^2$ caused a decrease in hardness on the material. The perfect atomic position is when exposed to ionic fire as an ion implantation process will cause atoms to detach from the bond while there is no more free space in the material. So that the released atoms will bounce and a new void appears. Finally, the metal surface becomes imperfect and is less able to withstand penetration from the outside. The decrease in the hardness can also be caused by the material experiencing saturation due to the spread of the layer to the side of the surface so that the surface is no longer an element of the nitride iron compound but only the nitrogen ion elements.

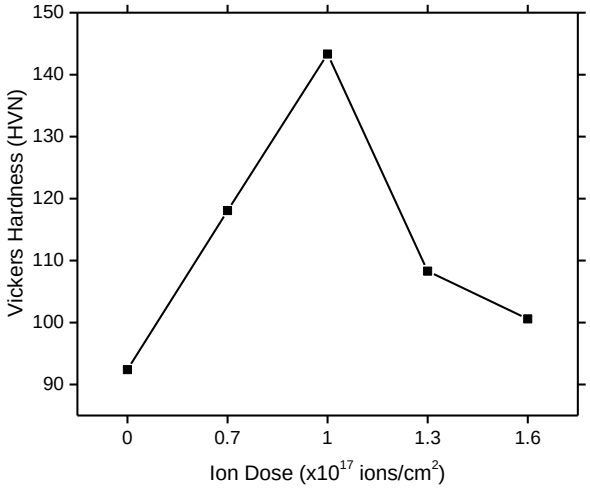


**Figure 2.** The graphic of the relationship between ion dosage variations on material hardnes

Potentiodynamic corrosion testing was performed to investigate the samples. Figure 3 showed the polarization resistance (*Rp*) austenitic SS 304 implanted with different nitrogen dosage ($0.7\times10^{17}$; $1.0\times10^{17}$; $1.3\times10^{17}$ and $1.6\times10^{17}$ ions/cm$^2$). The unimplanted materials were also tested for comparative purposes. An increase in the value of *Rp* in the implanted sample indicates an increase in the nitrogen [37]. Therefore, an increase in its properties was achieved. However, there is an unclear relationship in this experiment. The higher the dose of implantation, the decrease in polarization resistance value after the value of *Rp* reached the optimum peak. Other literature also found the same behavior, where the tendency with implantation doses could not be determined [30]. The decrease in *Rp* value also correlated with the decrease in hardness value. On the Rp optimum value occurred at the dosage $1.0\times10^{17}$ ions/cm$^2$, the value of material hardness also experienced an optimum increase. When the ion dose was raised $1.3\times10^{17}$ – $1.7\times10^{17}$ ions/cm$^2$, the *Rp* and hardness values encountered a decrease instead. This case signifies that the increase in material properties reached the optimum dosage and the next dosage addition would damage the previously formed nitride phase.

The Potentiodynamic anodic polarization curve from the unimplanted and implanted samples with nitrogen ion in the medium of SBF solution (Simulation Body Fluids) is presented in Figure 4. Based on the plot of the curve, it is shown that the corrosion potential ($E_{corr}$) of unimplanted and implanted samples is almost the same. On unimplanted material, the Potentiodynamic curve shows a passive region, but the main implant material at a dose of $1.0\times10^{17}$ ions/cm$^2$ of the sample had a more positive corrosion potential value. This case shows a better increase in corrosion resistance in implanted samples. The higher the Ecorr value of a material indicates the higher the corrosion resistance [38]. The higher corrosion resistance is considered originating from the implanted nitrogen ion [10].

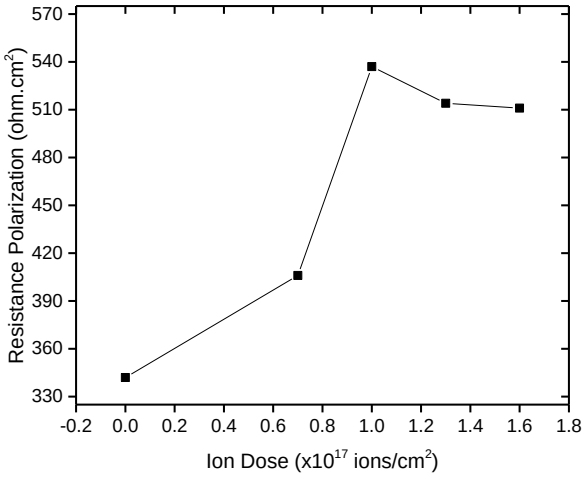


**Figure 3**. The resistance polarization of un-implanted and nitrogen implanted 304 SS

From the point of view of corrosion current density ($I_{corr}$), all implanted samples presented a superior corrosion resistance compared to the unimplanted ones. The measured $I_{corr}$ value shows a lot or at least metal ions dissolved in the electrolyte solution. If the current density is large, the soluble metal ion into the electrolyte solution is also large, indicating that there has been a greater corrosion rate and low corrosion resistance [22]. Based on the plot of the anodic polarization curve in Figure 4, it can be observed that the samples treated with $I_{coor}$ values were smaller than those without treatment. Therefore, it can be claimed that the nitride layer formed on stainless steel 304 can significantly increase corrosion resistance by inhibiting the occurrence of direct contact between corrosive ions and the surface of the sample. Literature studies also explain that the formation of nitride layers can also reduce the porosity between the constituent particles of the coating which leads to a smaller amount of moisture defects on the surface of the material so that the corrosion resistance of the material increases [37,38]. The value of corrosion current density and the corrosion rate is presented in Table 5.

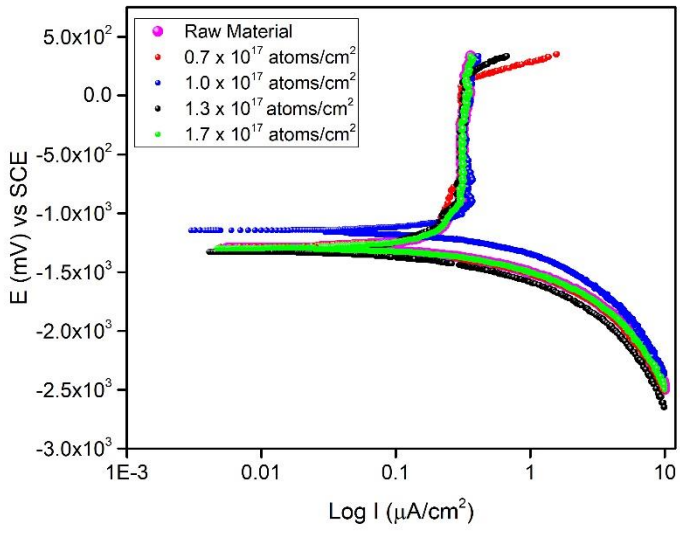


**Figure 4.** The Potentiodynamic polarization plots for un-implanted and nitrogen implanted 304 SS

**Table 5**. Corrosion current and corrosion rate of the sample

| Ion Dose (ions/cm$^2$) | Corrosion Current (μA/cm$^2$) | Corrosion Rate (mm/years) |
|---|---|---|
| Raw Material | 136.20 | 1.55 |
| $0.7\times10^{17}$ | 114.54 | 1.31 |
| $1.0\times10^{17}$ | 62.76 | 0.72 |
| $1.3\times10^{17}$ | 74.94 | 0.85 |
| $1.6\times10^{17}$ | 88.64 | 1.01 |

The calculation of corrosion rate used Equation 4 [31]. Where *CR* is corrosion rate (mm/year), *a* is atom mass (gram), *n* is valence electron, *I* is corrosion current (μA/cm$^2$), and *D* is material density (g/scm$^2$). The lower the corrosion rate of the material shows the greater its corrosion resistance is.

$$CR = 0.129\frac{aI}{nD} \tag{4}$$

Based on the calculation of corrosion rate as tabulated in Table 5, it can be observed at Figure 5 that the corrosion rate of the implanted sample is lower than the unimplanted sample. This case indicates that the nitride phase formed in the modified layer plays a very important role in increasing the corrosion resistance of the planted sample. The nitrogen ion implanted in the sample changes the surface topography by inducing defects in the sample to increase the corrosion resistance of the material [26]. The increased optimum corrosion resistance occurs at a dose of $1.0\times10^{17}$ ions/cm$^2$ reaching 0.72 mm / year. This case happens because nitrogen ions which are implanted in the target material lead to the arrangement of the atomic surface of a denser material. The dense arrangement of atoms makes the strength of the protective layer increase so that the corrosion rate decreases. However, if the implantation process is continuously carried out with the addition of a dose exceeding the requirement, there will be a deposit of nitrogen ions on the surface to form a thin amorphous layer [25]. The continuous addition of dosage will cause the ionic ion accumulated on the surface forming an amorphous layer thus the corrosion rate will increase.

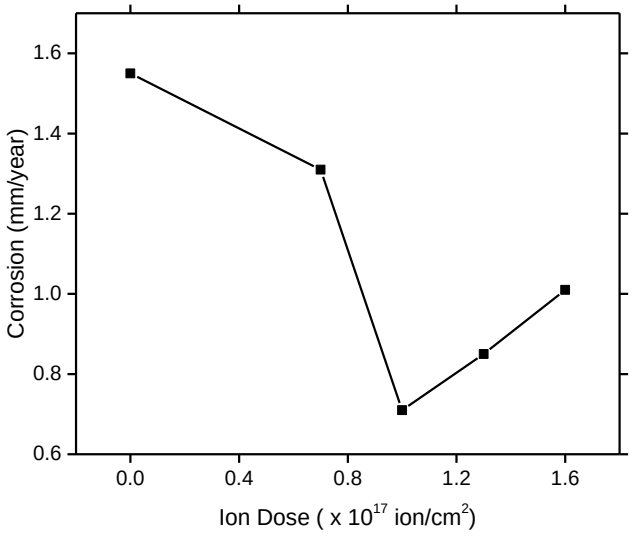


**Figure 5**. Corrosion result for un-implanted and implanted nitrogen 304 SS

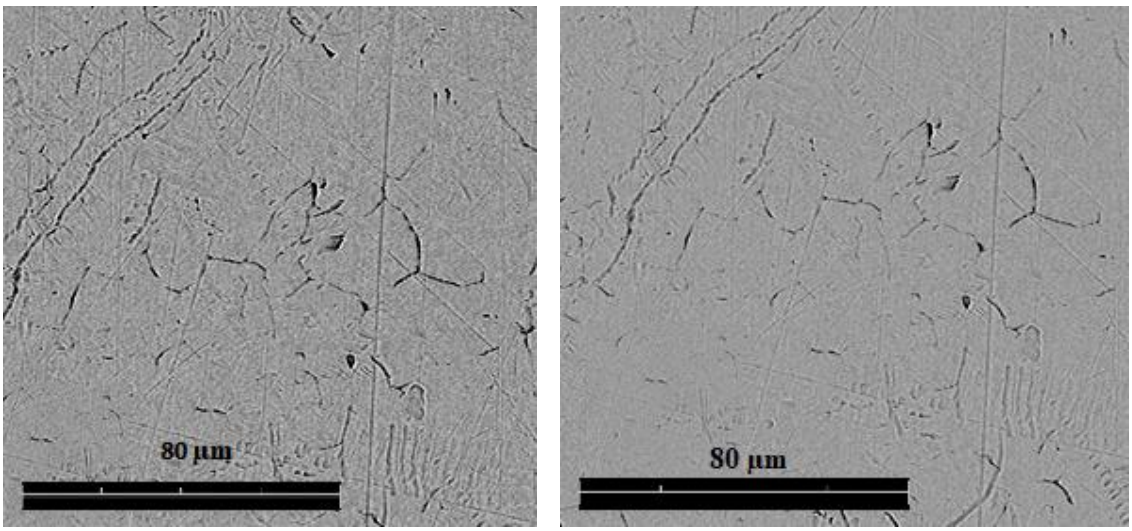


(a) (b)

**Figure 6**. SEM surface morphology nitrogen implanted 304L SS (a) Raw material (b) $1.0\times10^{17}$ ions/cm$^2$

The SEM image on the unimplanted and implanted samples is presented in Figure 6. The results of SEM-EDX testing were used as a support of the results of density testing, hardness testing, and corrosion rate testing. Based on these images, the changes in surface morphology were caused by ion implantation. Non-implantation samples were also tested for comparative purposes. The surface roughness of the implanted specimen appears to be larger than the implanted specimen. The effect of dispersing ions on the sample is considered to reduce surface roughness [41]. This happens because, in the sample that has not been implanted, the vacuum space in the sample has not been filled by the ion dopant. Meanwhile, the empty space in the sample undergoing the ion implantation process has been filled with nitrogen ions. Therefore, the density increased, and made the surface morphology look smoother. The penetration of ion tent to become interlatitudinal defect which as suspected to form a new balanced phase and will create a harder property and corrosion resistant on the material surface [26].

Regarding the composition of the sample element with EDX as illustrated in Table 6, it can be observed that there is an addition of nitrogen content from 3.4% on pure 304 SS becomes 5.2% on the implanted 304 SS. Based on the literature, the addition of nitrogen content must lead to the properties of hardness and corrosion of the material [11]. This case is possible because there was a phase change of Fe-N and Cr-, considering the composition of stainless steel 304 is dominated by Fe and Cr atoms. Literature studies also state the same thing that iron implanted with nitrogen at a certain percentage will form the nitride phase (Fe-N) [26]. This Fe-N phase has hardness properties. Meanwhile, the Cr-N phase will tend to resist corrosion because the implanted nitrogen ion inhibit Cr to react with easily oxidized Oxygen (Cr-O) [42].

**Table 6**. EDX from the nitrogen implanted 304L SS

| Composition | Weight percentage (Raw material) | Certainty | Weight percentage ($\times10^{17}$ ions/cm$^2$) | Certainty |
|---|---|---|---|---|
| Fe | 68.9 % | 0.99 | 66.5 % | 0.99 |
| Cr | 16.5 % | 0.99 | 15.1 % | 0.99 |
| Ni | 7.8 % | 0.96 | 7.8 % | 0.96 |
| N | 3.4 % | 0.94 | 5.2 % | 0.95 |
| C | 1.6 % | 0.85 | 4.2 % | 0.93 |
| Mn | 1.4 % | 0.90 | 1.0 % | 0.89 |
| Si | 0.4 % | 0.85 | 0.2 % | 0.77 |

## 4. Conclusion

The technic of nitrogen ion implantation has successfully increased the mechanical property of stainless steel 304. The SS 304 hardness has improved to 35% at the optimum dosage of $1.0\times10^{17}$ ions/cm$^2$ from the implant sample. The material density increased with the increase in implanted nitrogen ion. The corrosion rate also increased at the optimum dosage of $1.0\times10^{17}$ ions/cm$^2$. Interestingly, the decrease in corrosion rate reached 0.72 mm/year. The increase in hardness and the decrease in corrosion rate was caused by the formation of a new nitride layer on the sample surface due to the implantation process. This is shown in the results of SEM-EDX, the hardness of the ion implemented sample is smaller than the unimplanted one. This case is because the vacuum in the sample has been filled with implanted nitrogen ion. The addition of nitrogen ion in the results of EDX can increase the material density; thus the material can be harder and corrosion resistant.

## References

[1] Geetha M, Singh A K, Asokamani R and Gogia A K 2009 Ti based biomaterials, the ultimate choice for orthopaedic implants - A review *Prog. Mater. Sci.* **54** 397–425

[2] Kurtz S M, Lau E, Ong K, Zhao K, Kelly M and Bozic K J 2009 Future young patient demand for primary and revision joint replacement: National projections from 2010 to 2030 *Clin. Orthop. Relat. Res.* **467** 2606–12

[3] Bekmurzayeva A, Duncanson W J, Azevedo H S and Kanayeva D 2018 Surface modification of stainless steel for biomedical applications: Revisiting a century-old material *Mater. Sci. Eng. C*

[4] Xiao M, Chen Y M, Biao M N, Zhang X D and Yang B C 2017 Bio-functionalization of biomedical metals *Mater. Sci. Eng. C* **70** 1057–70

[5] Grayeli-Korpi A R and Savaloni H 2012 Effect of nitrogen ion implantation on corrosion inhibition of nickel coated 316 stainless steel and correlation with nano-structure *Appl. Surf. Sci.* **258** 9982–8

[6] Rodriguez-Contreras A, Guadarrama Bello D, Flynn S, Variola F, Wuest J D and Nanci A 2018 Chemical nanocavitation of surfaces to enhance the utility of stainless steel as a medical material *Colloids Surfaces B Biointerfaces* **161** 677–87

[7] Mulyaningsih N, Salahudin X, Iswanto P T and Soekrisno 2014 Analisis Perbandingan Laju Korosi Material Ss 304 Lapis Ni-Cr Dengan Ss 316 L Teriiadap Pengaruh Cairan Tubuh Nani *Univ. Tidar Magelang* **40** 95–107

[8] Panahi H, Eslami A and Golozar M A 2018 Corrosion and stress corrosion cracking initiation of grade 304 and 316 stainless steels in activated Methyl Diethanol Amine (aMDEA) solution *J. Nat. Gas Sci. Eng.* **55** 106–12

[9] Shi L, Iwamoto T and Hashimoto S 2013 An Experimental Study on Rate Sensitivity of J - Integral and its Evaluation by Small Punch Test for TRIP Steel 119–36

[10] Li Y, He Y, Zhang S, Wang W and Zhu Y 2018 Microstructure and corrosion resistance of nitrogen-rich surface layers on AISI 304 stainless steel by rapid nitriding in a hollow cathode discharge *Appl. Phys. A Mater. Sci. Process.* **124** 1–10

[11] Bhuyan H, Mändl S, Bora B, Favre M, Wyndham E, Maze J R, Walczak M and Manova D 2014 Surface modification by nitrogen plasma immersion ion implantation into new steel 460Li-21Cr in a capacitively coupled radio frequency discharge *Appl. Surf. Sci.* **316** 72–7

[12] Cui X, Wang L, Shen J, Zhong H, Zhang J, Liang G, Yu X, Zhang X and Le X 2018 Lattice damage and expansion in RbTiOPO4crystals induced by carbon ion implantation *Surf. Coatings Technol.* **348** 142–9

[13] Stepanov A L, Nuzhdin V I, Valeev V F, Rogov A M, Vorobev V V. and Osin Y N 2018 Porous germanium formed by low energy high dose Ag+-ion implantation *Vacuum* **152** 200–4

[14] Narojczyk J, Morozow D, Narojczyk J W and Rucki M 2018 Ion implantation of the tool's rake face for machining of the Ti-6Al-4V alloy *J. Manuf. Process.* **34** 274–80

[15] Rahman M and Hashmi M S J 2006 Effect of treatment time on low temperature plasma nitriding of stainless steel by saddle field neutral fast atom beam source *Thin Solid Films* **515** 231–8
[16] Rahman M, Haider J and Hashmi M S J 2005 Low temperature plasma nitriding of 316 stainless steel by a saddle field fast atom beam source *Surf. Coatings Technol.* **200** 1645–51
[17] Kereszturi K, Szabó A, Tóth A, Marosi G and Szépvölgyi J 2008 Surface modification of poly(tetrafluoroethylene) by saddle field fast atom beam source *Surf. Coatings Technol.* **202** 6034–7
[18] Liao H B, Wen W and Wong G K L 2003 Preparation and optical characterization of Au/SiO[sub 2] composite films with multilayer structure *J. Appl. Phys.* **93** 4485
[19] Liang G X, Zheng Z H, Fan P, Luo J T, Hu J G, Zhang X H, Ma H L, Fan B, Luo Z K and Zhang D P 2018 Thermally induced structural evolution and performance of Sb2Se3films and nanorods prepared by an easy sputtering method *Sol. Energy Mater. Sol. Cells* **174** 263–70
[20] Kashiwaba Y, Tanaka Y, Sakuma M, Abe T, Imai Y, Kawasaki K, Nakagawa A, Niikura I, Kashiwaba Y and Osada H 2018 Preparation of a Non-Polar ZnO Film on a Single-Crystal NdGaO3 Substrate by the RF Sputtering Method *J. Electron. Mater.* **47** 4345–50
[21] Jasinski J J, Fraczek T, Kurpaska L, Lubas M and Sitarz M 2018 Investigation of nitrogen transport in active screen plasma nitriding processes e Uphill diffusion effect *J. Mol. Struct.* **1164** 37–44
[22] Taherkhani K and Soltanieh M 2018 Composite coatings created by new method of active screen plasma nitriding on aluminium alloy 6061 *J. Alloys Compd.* **741** 1247–57
[23] Lin K, Li X, Sun Y, Luo X and Dong H 2014 Active screen plasma nitriding of 316 stainless steel for the application of bipolar plates in proton exchange membrane fuel cells *Int. J. Hydrogen Energy* **39** 1–10
[24] Sioshansi P 1989 Surface modification of industrial components by ion implantation *Nucl. Inst. Methods Phys. Res. B* **37**–**38** 667–71
[25] Jedi-Soltanabadi Z, Ghoranneviss M, Ghorannevis Z and Akbari H 2018 Effect of Ti Substrate Ion Implantation on the Physical Properties of Anodic $TiO_2$ Nanotubes *J. Korean Phys. Soc.* **72** 604–9
[26] Ueda M, Silva M M, Otani C, Reuther H, Yatsuzuka M, Lepienski C M and Berni L A 2003 Improvement of tribological properties of Ti6Al4V by nitrogen plasma immersion ion implantation *Surf. Coatings Technol.* **169** 408–10
[27] Öztürk O 2009 Microstructural and mechanical characterization of nitrogen ion implanted layer on 316L stainless steel *Nucl. Instruments Methods Phys. Res. Sect. B Beam Interact. with Mater. Atoms* **267** 1526–30
[28] Kliauga A M, Pohl M and Klaffke D 1998 Ti A comparison of the friction and reciprocating wear behaviour between **02** 237–44
[29] Lanning B R and Wei R 2004 High intensity plasma ion nitriding of orthopedic materials. Part II. Microstructural analysis *Surf. Coatings Technol.* **186** 314–9
[30] Castro-Colin M, Durrer W, López J A and Ramirez-Homs E 2016 Surface Modification by Nitrogen Plasma Immersion Ion Implantation on Austenitic AISI 304 Stainless Steel *J. Iron Steel Res. Int.* **23** 380–4
[31] Shen L R, Wang K, Tie J, Tong H H, Chen Q C, Tang D L, Fu R K Y and Chu P K 2005 Modification of high-chromium cast iron alloy by N and Ti ion implantation *Surf. Coatings Technol.* **196** 349–52
[32] Padhy N, Ningshen S, Panigrahi B K and Mudali U K 2010 Corrosion behaviour of nitrogen ion implanted AISI type 304L stainless steel in nitric acid medium *Corros. Sci.* **52** 104–12
[33] Istiyono E 2004 *Implantasi Ion sebagai Upaya Modifikasi Sifat Mekanik dan Elektrik Bahan Prosiding Seminar Nasional Penelitian, Pendidikan dan Penerapan MIPA* 41–50
[34] Pratesa Y, Harjanto S, Larasati A, Suharno B and Ariati M 2018 Degradable and porous Fe-Mn-C alloy for biomaterials candidate *AIP Conf. Proc.* **1933**

[35] Jatisukamto G, Malau V, Ilman M N and Iswanto P T 2011 Perbaikan Sifat Korosi Baja Tahan Karat AISI 410 Dengan Perlakuan Implantasi Ion Tin **5** 14–9
[36] William D. Callister J and David G. Rethwisch 2010 Materials science and engineering: An introduction *Mater. Des.* 885
[37] Somasundaram S, Ionescu M and Mathan B 2018 Ion Implantation of Calcium and Zinc in Magnesium for Biodegradable Implant Applications *Metals (Basel).* **8** 30
[38] Zhang F, Yan M, Yin F, Wang Y, Zhang Y and He J 2018 Influence of plasma nitriding temperature on microstructures and mechanical properties of Ti-N/Ti-Al multilayer coatings on the surface of 5083 Al alloys *Surf. Coatings Technol.* **335** 80–7
[39] Shanaghi A, Rouhaghdam A R S, Ahangarani S and Chu P K 2012 Effect of plasma CVD operating temperature on nanomechanical properties of TiC nanostructured coating investigated by atomic force microscopy *Mater. Res. Bull.* **47** 2200–5
[40] Raoufi M, Mirdamadi S, Mahboubi F, Ahangarani S, Mahdipoor M S and Elmkhah H 2011 Correlation between the surface characteristics and the duty cycle for the PACVD-derived TiN nanostructured films *Surf. Coatings Technol.* **205** 4980–4
[41] Kim K and Jeong J H 2018 Condensation mode transition and condensation heat transfer performance variations of nitrogen ion-implanted aluminum surfaces *Int. J. Heat Mass Transf.* **125** 983–93
[42] Ryabchikov A, Sivin D, Ananin P, Ivanova A, Lopatin I, Korneva O and Shevelev A 2018 High intensity, low ion energy implantation of nitrogen in AISI 5140 alloy steel *Surf. Coatings Technol.*